J. Materials, Conc. Struct., Pavements No. 502/V-25, pp. 143~154, November 19

CONSTITUTIVE MODELS OF CONCRETE UNDER PASSIVE CONFINEMENT AND THEIR USE IN STRUCTURAL ANALYSIS

Masanori KINOSHITA*, Milija N. PAVLOVIĆ** and Michael D. KOTSOVOS***

When a concrete cylinder is confined laterally by a steel tube, or it is strongly reinforced with closely-spaced hoop reinforcement bars, the axial strength and ductility of concrete are improved considerably. In such structures, large confining pressures are passively induced by steel due to the lateral expansion of concrete.

The present paper proposes a constitutive model for describing the multiaxial deformational behaviour of concrete under passive confinement by using the work-hardening elasto-plasticity theory. The derivation of the proposed model is based on the use of experimental information obtained from tests in which concrete has been subjected to passive confinement. A computer program for finite-element (FE) analysis based on the use of the proposed model has been developed. The FE analysis successfully predicted the load-carrying capacities and deformational responses of concrete-filled composite columns subjected to eccentric loading.

Key Words: *confined concrete, constitutive model, plasticity, finite-element analysis*

1. INTRODUCTION

When a concrete cylinder is confined laterally by a steel tube, or it is strongly reinforced with closely-spaced hoop reinforcement bars, the axial strength and ductility of concrete are improved considerably. In such structures, large confining pressures are passively induced by steel due to the lateral expansion of concrete.

Stress-strain relationships and ultimate strength envelopes under multiaxial stress states have been usually investigated by testing cylinders or cubes under active confinement, in which the stress paths are controlled in a prescribed manner. A common stress path is described in **Fig.1** (see path (a)), in which a deviatoric stress states is applied while pure hydrostatic pressure having increased to a given value remains constant. However, such information obtained from the above active type of testing is not sufficient for modelling the behaviour of concrete passively confined by steel reinforcement. In fact, it is a generally held view that the constitutive relations of concrete established in the past from tests with active confinement are practically incapable of describing the behaviour

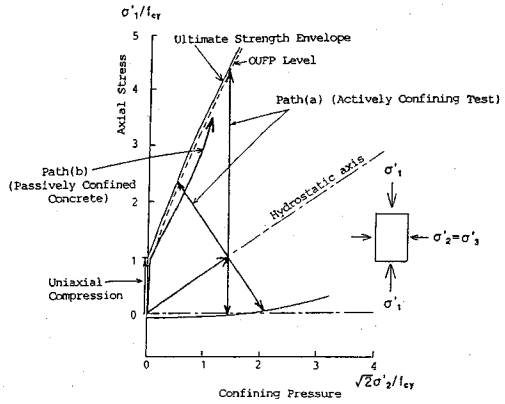

Fig.1 Stress paths of general triaxial tests and passively confined concrete

of concrete under passive confinement. This is due to the differences in stress paths which concrete experiences in between ordinary active type of tests and a passively confined portion of concrete in practical structures[2] (see **Fig.1** path (b)), because the properties of concrete distinctly change when the minimum volume level is attained with the stresses increasing in an almost uniaxial manner[2]. The minimum volume level is termed the"onset of unstable fracturing process"or OUFP. The OUFP level lies around 90% of the uniaxial strength of concrete under uniaxial compression[2].

From the above viewpoint, the authors conducted a series of experiments to investigate the deformational behaviour of concrete beyond the

*Member of JSCE, Ph.D., Senior Researcher, Nippon Steel Corporation
(20-1 Shintomi, Futtsu, Chiba, 293 Japan)
**Ph.D., Reader, Imperial College of Science, Technology and Medicine, London
***Ph.D., Professor, National Technical University of Athens, Athens

OUFP level under passive confinement[2]. The present paper is aimed at using the information obtained from the tests as the basis of an attempt to derive a constitutive model capable of describing the behaviour of concrete subjected to passive confinement. In other words, the objective of the present paper is modelling the concrete behaviour after the OUFP level is once attained.

2. CHARACTERISTIC FEATURES OF POST-OUFP CONCRETE AND MODELLING TECHNIQUES

A number of techniques have been proposed to date for the modelling of the deformational response of materials. The complexity of the behaviour of concrete under multiaxial states of stress is such that it has so far prevented the development of a constitutive model that is both simple and accurate. The modelling of concrete behaviour is heavily dependent on the characteristic features which are to be modelled. Prior to the modelling of post–OUFP behaviour of concrete, therefore, these characteristic features must be identified.

The experimental information obtained from the tests on passively confined concrete[2] has clarified some of the most important characteristic features of the post–OUFP behaviour of passively confined concrete.

(1) Elastic properties: First of all, the elastic properties expressed in the form of shear and bulk moduli experience distinct changes for stress levels beyond the OUFP level. In particular, the shear modulus is severely damaged to less than 50% of that of the original concrete.

(2) Ultimate strength envelope: The ultimate strength envelope established from a test with active confinement is not valid for passively confined concrete. It was found that, once the OUFP level is exceeded, the ultimate strength envelope becomes dependent on the mix design; the higher the uniaxial strength of concrete, the smaller the ultimate strength envelope expressed in a normalized form with respect to the uniaxial compression strength.

(3) Dilational behaviour near ultimate strength: Significant dilational behaviour is observed when the stress states reach close to the ultimate strength envelope. The dilational behaviour is very sensitive to the hydrostatic pressure applied. The higher the hydrostatic pressure, the less pronounced the dilational behaviour just before the ultimate strength envelope. As the dilational behaviour (i. e., the significant development of transverse strains) causes the multiaxial stress states in actual structures, it is very important for modelling the post–OUFP concrete.

(4) Ductility: Although plain concrete itself is essentially a very brittle fracturing material, post–OUFP concrete behaves in a very ductile manner when the material is passively confined. The development of confining pressure increases ductility significantly as well as the load carrying capacity. In addition, the strain at the ultimate state is significantly sensitive to hydrostatic pressure. The larger the hydrostatic pressure, the larger the total strain at the ultimate strength envelope. This feature of post–OUFP concrete is considered to result in the ductile behaviour of concrete structures.

The last two features of the deformational behaviour are the more characteristic of post–OUFP concrete behaviour when comparing them with those of plain concrete below OUFP levels. The close description of the ductile behaviour of concrete under passive confinement is dependent to a large extent on the successful modelling of the above features of the post–OUFP behaviour of concrete, as the volume change causes the multiaxial stress states and this affects the ductility of the material. Therefore, much attention has to be focused into modelling the above features.

3. MODELLING OF POST-OUFP CONCRETE BEHAVIOUR BY ELASTO-PLASTICITY THEORY

In this section, an elasto–plasticity model for the post–OUFP behaviour is derived by using only the information obtained from the previous experimental work described in Ref 2). In order to derive the elasto–plastic model, we have to formulate the loading functions representing the loading surfaces, and the plastic potential functions defining the direction of the incremental plastic strains.

(1) A proposed loading function

The objective in this section is to derive the mathematical expression which provides a realistic description of the loading surfaces. If plastic work is assumed only a hardening parameter, contour lines of plastic work experimentally obtained give an image of loading surfaces. From the observation of the contour lines, it is found that a cap–model[3], which comprises a strength envelope and a cap function, forms a suitable basis for developing a model for the present material. The cap model is, in principle, capable of describing the significant sensitivity of ductility to hydrostatic pressure. Having considered the capability of the function to provide a realistic representation of the contour lines of plastic work experimentally obtained, the following expression is recommended as a cap–function:

$$f(\sigma'_{ij}, P)=\left(\frac{\sigma'_0/f_{cy}+S}{P}\right)^{b1}-\left(\frac{\sigma'_0/f_{cy}+S}{P}\right)^{b0}+\left(\frac{\tau'_0/f_{cy}}{A}\right)^2=0 \quad \cdots\cdots(1)$$

where f_{cy} is a cylinder strength of concrete, σ'_0, τ'_0 are octahedral normal and shear stresses, S, $b1$, $b0$ and A are constants and P is a hardening parameter which is assumed to be a function of plastic work. In equation (1), constants $b1$ and $b0$ basically determine the shape of the ellipse-like surface defined by the equation. For example, when $b1=2$ and $b0=1$ are chosen, the intersection of the surface with the octahedral plane is a perfect ellipse. In order to reduce the number of unknown constants, the condition that a cap function should smoothly connect the strength envelope is imposed, which means that the tangent of the surface at the intersection with the strength envelope corresponds to that of the strength envelope. The following type of expression for the strength envelopes has already been proposed in Ref 2):

$$\tau'_0/f_{cy}=k_f(\sigma'_0+s'_f)^{\alpha} \quad \cdots\cdots(2)$$

where k_f, s_f and α are material constants

When A and S in equation (1) are chosen so as to satisfy the expression,

$$A=\frac{k_f\left(\frac{b0-2\alpha}{b1-2\alpha}\right)^{\alpha/(b1-b0)}}{\sqrt{\left(\frac{b0-2\alpha}{b1-2\alpha}\right)^{b0/(b1-b0)}-\left(\frac{b0-2\alpha}{b1-2\alpha}\right)^{b1/(b1-b0)}}}P^{\alpha} \quad (3)$$

and $S=s_f$

then equation (1) smoothly connects equation (2) at the intersection. That is:

$$For\ \frac{\sigma'_0/f_{cy}+S}{P}\geq\left(\frac{b0-2\alpha}{b1-2\alpha}\right)^{1/(b1-b0)}$$

$$f(\sigma'_{ij}, P)=\left(\frac{\sigma'_0/f_{cy}+S}{P}\right)^{b1}-\left(\frac{\sigma'_0/f_{cy}+S}{P}\right)^{b0}+\left(\frac{\tau'_0/f_{cy}}{KP^{\alpha}}\right)^2=0 \quad \cdots\cdots(4)$$

$$For\ \frac{\sigma'_0/f_{cy}+S}{P}\leq\left(\frac{b0-2\alpha}{b1-2\alpha}\right)^{1/(b1-b0)}$$

$$f(\sigma'_{ij}, P)=\tau'_0/f_{cy}-k_f(\sigma'_0/f_{cy}+s_f)^{\alpha}=0 \quad \cdots\cdots(5)$$

where

$$K=\frac{k_f\left(\frac{b0-2\alpha}{b1-2\alpha}\right)^{\alpha/(b1-b0)}}{\sqrt{\left(\frac{b0-2\alpha}{b1-2\alpha}\right)^{b0/(b1-b0)}-\left(\frac{b0-2\alpha}{b1-2\alpha}\right)^{b1/(b1-b0)}}} \quad \cdots(6)$$

and $S=S_f$

In the above loading function, the unknown constants are only $b1$ and $b0$. It can be easily deduced by inspection of the function that the difference of the two constants (i. e., $b1-b0$) mainly governs the shape of the surface, while the constant $b0$ affects the position where the loading surface intersects the strength envelope. The hardening parameter P governs the size of the surface.

On the other hand, a loading surface should expand in relation to the plastic work W^P. Therefore, P should be definable in relation to W^P, independently of the stress path in the course of monotonic loading. P is assumed to be related to the work W^P by:

$$P\,dP=h(W^P)\,dW^P=h(W^P)\,\sigma'_{ij}\,d\varepsilon^P_{ij} \quad \cdots\cdots(7)$$

or

$$\frac{1}{2}P^2=H(W^P) \quad \cdots\cdots(8)$$

where $h(W^P)=\frac{\partial H}{\partial W^P}$ is a hardening function

Once $b1$ and $b0$ in equation (4) are chosen, the relation between W^P and $1/2P^2$ can be established for each case tested (i. e., stress path). However, the relation must be independent of stress path, if equation (4) is to be a true loading function. Consequently, $b1$ and $b0$ should be chosen from experimental data so that the relation between W^P and $1/2P^2$ is essentially independent of stress path. The procedure to determine optimum values for $b1$ and $b0$ is as follows: **a**) calculate the relation between W^P and $1/2P^2$ along each tested path for given $b1$ and $b0$, **b**) fit a parabolic curve to the data W^P, $1/2P^2$ so that the residue defined by equation (9) below becomes a minimum, **c**) repeat a) and b) for various combinations of $b1$ and $b0$, **d**) finally, choose the optimum $b1$ and $b0$ (i. e., with the minimum residue).

$$residue=\sum_1^n\left(\frac{1/2P^2-r(W^P)}{1/2P^2}\right)^2\rightarrow\min \quad \cdots\cdots(9)$$

where n=number of data

$r(W^P)=a_2W^{P2}+a_1W^P+a_0$

(parabolic regression curve)

(a_2, a_1, a_0 are constants to be determined)

The material constants thus obtained from the tests[2] are tabulated in **Table 1.**

Table 1 Material constants for loading function

The hardening function $h(W^P)$ is defined as follows:

$h(W^P)=1.982+0.673W^P$ (for the mix of f_{cy}=33MPa) ·····(10)

$h(W^P)=1.293+0.038W^P$ (for the mix of f_{cy}=45MPa) ·····(11)

Figs.2 and **3** show graphical representations of the loading functions defined above. In the figures,

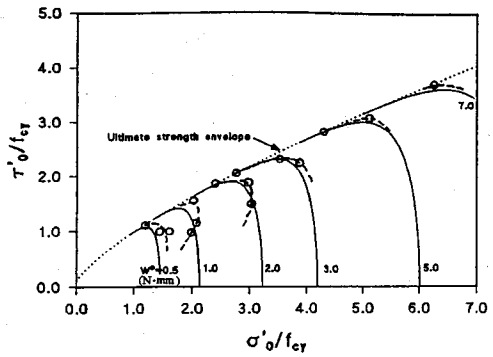

Fig.2 Loading surface proposed for the mix of f_{cy} =33MPa

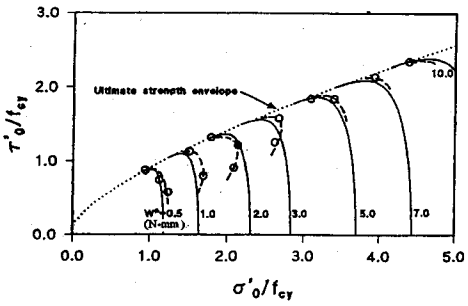

Fig.3 Loading surface proposed for the mix of f_{cy} =45MPa

solid lines are the loading surface defined by equation (4) while break lines are experimentally obtained contour lines of plastic work (W^P). It may be seen that equation (4) yields a good approximation to the loading surfaces which describe the contour lines of plastic work.

(2) A proposed plastic potential function

A plastic potential function defines the direction of plastic flow as follows:

$$d\varepsilon^P_{ij}=d\lambda \frac{\partial g}{\partial \sigma_{ij}} \quad \cdots\cdots(12)$$

Equation (12) implies that incremental vectors of plastic strains $d\varepsilon^P_{ij}$ are perpendicular to surfaces defined by a plastic potential function $g\ (\sigma'_{ij})$. In other words, to define a plastic potential function is to find a mathematical expression defining the surfaces which are always, at any point in a stress space, perpendicular to the incremental vectors of plastic strains obtained from previous tests. Therefore, the successful modelling of the dilational behaviour of the post-OUFP concrete is dependent upon an adequate definition of plastic potential function. Under an associated flow rule, a plastic potential function is assumed to be identical to a yield function. However, the experimental results presented indicate that post-OUFP concrete follows a non-associated flow rule. As a result, a plastic potential function should be defined as an expression independent of a yield function.

A clear signpost of the plastic strain behaviour of post-OUFP concrete is a critical line where no plastic volumetric change occurs. Therefore, a tangential line on surfaces defined in an octahedral stress space by a potential function should be, at any point on the critical line, parallel to the normal octahedral stress axis. In order to comply with the condition that a tangent of the surface must be zero at any point on the critical line whose expression has been proposed in Ref 2) as

$$\tau'_0/f_{cy}=k_c\ (\sigma'_0/f_{cy})^{\alpha c} \quad \cdots\cdots(13)$$

where k_c and α_c are material constants.

We choose as a plastic potential function a similar expression to the loading function established in the preceding section:

$$g\ (\sigma'_{ij})=\left(\frac{\sigma'_0/f_{cy}+s_f}{Q+C}\right)^{d1}-\left(\frac{\sigma'_0/f_{cy}+s_f}{Q+C}\right)^{d0}+\left(\frac{\tau'_0/f_{cy}}{K_0\ Q^{\alpha}}\right)^2=0 \quad \cdots\cdots(14)$$

where

$$C=\frac{s_f}{\left(\frac{d0}{d1}\right)^{1/(d1-d0)}} \quad \cdots\cdots(15)$$

$$K_0=\frac{k_c\left(\frac{d0}{d1}\right)^{d/(d1-d0)}}{\sqrt{\left(\frac{d0}{d1}\right)^{d0/(d1-d0)}-\left(\frac{d0}{d1}\right)^{d1/(d1-d0)}}} \quad \cdots\cdots(16)$$

and Q is a parameter defined by a corresponding stress state, which can be obtained by simply solving equation (14). The potential function can be defined by choosing constants $d1$ and $d0$ so as to fit experimental data as closely as possible. Now, the shape of the surface is not significantly sensitive to the constant $d0$, while it is very sensitive to the difference of the two constants (i. e., $d1-d0$). Therefore, in order to reduce the number of unknown constants, $d0=2\alpha_c$ is chosen for the value of $d0$, which does not affect the overall performance of the potential function:

$$d0=2\alpha_c \quad \cdots\cdots(17)$$

As the direction of plastic strains changes slowly below the critical line, but rapidly above the line, it is a good idea to choose different constants $d1$ above and below the critical line respectively. A constant $d1$ may be assessed by an iterative (trial and error) method, similar to that used to define the loading surfaces, which makes use of the experimental data so that the residue defined by the following equation:

Table 2 Material constants for plastic potential function

Material	*d1*	*d0*	k_c	α_c
f_{cy}=33MPa	22.0 (above CL*) 1.7 (below CL*)	1.480	0.942	0.740
f_{cy}=45MPa	17.0 (above CL*) 1.6 (below CL*)	1.344	0.872	0.672

(*CL stands for critical line)

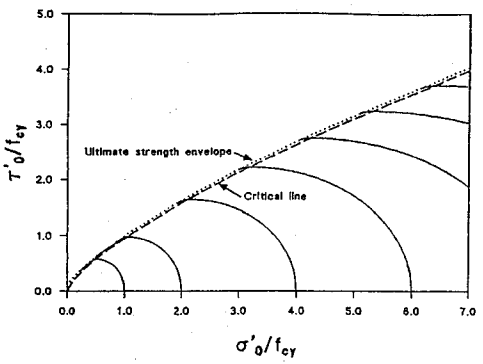

Fig.4 Plastic potential function proposed for the mix of f_{cy}=33MPa

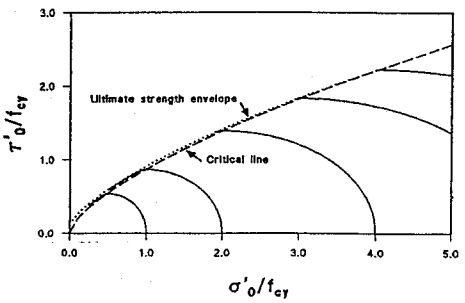

Fig.5 Plastic potential function proposed for the mix of f_{cy}=45MPa

$$residue=\frac{\sum_{1}^{n}\left(\sum_{i=1}^{n}\frac{|v_p\otimes(\overrightarrow{\partial g/\partial\sigma})|}{|v_p||(\overrightarrow{\partial g/\partial\sigma})v_p|}\right)^{n}}{N}\rightarrow\min \quad (18)$$

where

$\overrightarrow{v_P}$=vectors of plastic flow obtained by experiments

$(\overrightarrow{\partial g/\partial\sigma})$ =vectors normal to a given plastic potential function

$|\overrightarrow{a}|$ =an absolute value (or length) of a vector $\overrightarrow{a}$

$\overrightarrow{a}\otimes\overrightarrow{b}$=vector product of $\overrightarrow{a}$ and $\overrightarrow{b}$

n=number of data in each path

N=number of path tested

becomes a minimum. From the analysis of residues, the material constants are tabulated in **Table 2**. **Figs 4** and **5** show the surfaces defined by the potential function. The curves represented by the functions above and below the critical line are smoothly connected to each other on the critical line, because the tangents of the surfaces defined by equation (13) are zero on any point on the critical line.

(3) Incremental description of constitutive relations of passively confined concrete

In plasticity theory, total strains $d\varepsilon_{ij}$ are considered to comprise elastic strains $d\varepsilon^e_{ij}$ and plastic strains $d\varepsilon^P_{ij}$:

$$d\varepsilon_{ij}=d\varepsilon^e_{ij}+d\varepsilon^P_{ij} \quad (19)$$

The elastic response is governed by the generalized law of Hooke as follows :

$$d\sigma_{ij}=D^e_{ijkl}d\varepsilon^e_{kl} \quad (20)$$

where D^e_{ijkl} is the elastic stiffness tensor of the material.

When the loading and plastic potential functions are defined, incremental stress-strain relationships can be expressed as follows[3]:

$$d\sigma_{ij}=(D^e_{ijkl}+D^P_{ijkl})\ d\varepsilon_{kl} \quad (21)$$

where

$$D^P_{ijkl}=-\frac{D^e_{ijtu}(\partial g/\partial\sigma_{tu})(\partial f/\partial\sigma_{rs})D^e_{rskl}}{h+(\partial f/\partial\sigma_{mn})D^e_{mnpq}(\partial g/\partial\sigma_{pq})} \quad (22)$$

$$h=-\frac{\partial f}{\partial\varepsilon^P_{ij}}\frac{\partial g}{\partial\sigma_{ij}}-\frac{\partial f}{\partial P}\frac{\partial P}{\partial\varepsilon^P_{ij}}\frac{\partial g}{\partial\sigma_{ij}} \quad (23)$$

P: hardening parameter

From equation (4),

$$\frac{\partial f}{\partial\sigma'_{ij}}=\frac{1}{3f_{cy}P}\left\{b1\left(\frac{\sigma'_0/f_{cy}+S}{P}\right)^{b1-1}-b0\left(\frac{\sigma'_0/f_{cy}+S}{P}\right)^{b0-1}\right\}\delta_{ij}+\frac{2}{3}\left(\frac{1/f_{cy}}{KP^{\alpha}}\right)^2 s'_{ij}$$
$$=A_f\delta_{ij}+B_f s'_{ij} \quad (24)$$

$$\frac{\partial f}{\partial P}=-\frac{1}{P}\left\{b1\left(\frac{\sigma'_0/f_{cy}+S}{P}\right)^{b1}-b0\left(\frac{\sigma'_0/f_{cy}+S}{P}\right)^{b0}+2\alpha\left(\frac{\tau'_0/f_{cy}}{KP^{\alpha}}\right)^2\right\}$$
$$=C_f \quad (25)$$

where

δ_{ij}=Kronecker's delta (when $i=j$, $\delta_{ij}=1$. when $i\neq j$, $\delta_{ij}=0$)

s'_{ij}=deviatoric stress tensor=$\sigma'_{ij}-\sigma'_0\delta_{ij}$

From equation (10),

$$\frac{\partial g}{\partial\sigma'_{ij}}=\frac{1}{3f_{cy}(Q+C)}\left\{d1\left(\frac{\sigma'_0/f_{cy}+S}{Q+C}\right)^{d1-1}-d0\left(\frac{\sigma'_0/f_{cy}+S}{Q+C}\right)^{d0-1}\right\}\delta_{ij}+\frac{2}{3}\left(\frac{1/f_{cy}}{K_0Q^{\alpha}}\right)^2 s'_{ij}$$
$$=M_F\delta_{ij}+N_F s'_{ij} \quad (26)$$

On the other hand, for an isotropic elastic material, the elastic stiffness tensor is

$$D^e_{ijkl}=\lambda\delta_{ij}\delta_{kl}+\mu\ (\delta_{ik}\delta_{jl}+\delta_{il}\delta_{jk}) \quad (27)$$

where λ, μ are Lame's constants

Lame's constants are related to the bulk and shear

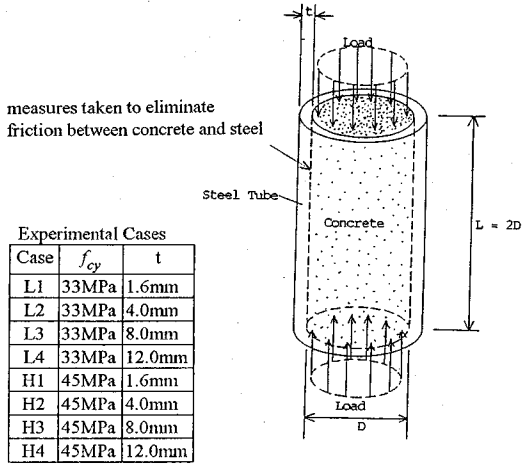

Experimental Cases

Case	f_{cy}	t
L1	33MPa	1.6mm
L2	33MPa	4.0mm
L3	33MPa	8.0mm
L4	33MPa	12.0mm
H1	45MPa	1.6mm
H2	45MPa	4.0mm
H3	45MPa	8.0mm
H4	45MPa	12.0mm

f_{cy}:Cylinder strength of concrete used
t:Thickness of steel tube used
D=88.9mm:Diameter of concrete

Fig.6 Description of testing[2)]

moduli (K_e, G_e) as follows:

$$\lambda=\frac{3K_e-2G_e}{3} \quad \cdots\cdots(28)$$

$$\mu=G_e$$

Therefore,

$$\frac{\partial f}{\partial \sigma'_{kl}} D^e_{klij}=D^e_{ijkl}\frac{\partial f}{\partial \sigma'_{kl}}=A_f\ (3\lambda+2\mu)\ \delta_{ij}+2B_f\mu s'_{ij} \quad \cdots\cdots(29)$$

$$\frac{\partial g}{\partial \sigma'_{kl}} D^e_{klij}=D^e_{ijkl}\frac{\partial g}{\partial \sigma'_{kl}}=M_P\ (3\lambda+2\mu)\ \delta_{ij}+2N_P\mu s'_{ij} \quad \cdots\cdots(30)$$

By substituting equations (24) to (27) into (22) and (26), and by using the hardening function $h\ (W^P)$ defined in the previous section, a plastic stiffness tensor is obtained:

$$D^P_{ijkl}=-\frac{(M_P(3\lambda+2\mu)\delta_{ij}+2N_P\mu s'_{ij})(A_f(3\lambda+2\mu)\delta_{kl}+2B_f\mu s'_{kl})}{\bar{\sigma}^2}$$

where

$$\bar{\sigma}^2=-C_f\frac{h(W^P)}{P}\ (3M_P\sigma'_0+3N_P\tau'^2_0)+3A_fM_P\ (3\lambda+2\mu)+6B_fN_P\tau'^2_0 \quad \cdots\cdots(31)$$

(5) Verification of the validity of the proposed model

In this section, the results obtained from the experiments described in Ref 2) are to be reproduced numerically by using the constitutive model proposed, in order to verify the validity of the model. In the experiments, concrete cast in short steel tubes was subjected to compression (see **Fig 6**). In the analyses, it is assumed that there is no friction between concrete and steel tube, because the effect of friction on the obtained results has been allowed for by the calculation in Ref 2).

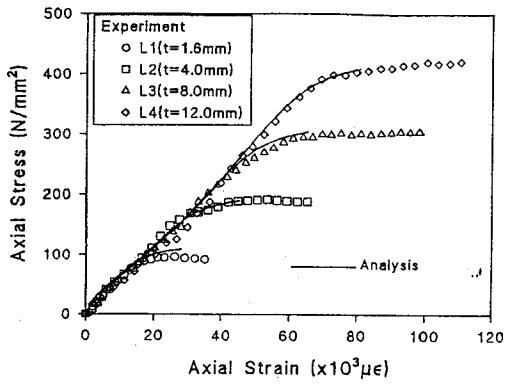

Fig.7 Comparison of analysis with the experimental data--Stress–strain curves for the mix of f_{cy} =33MPa--

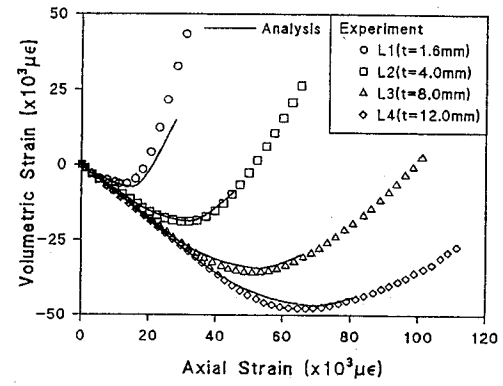

Fig.8 Comparison of analysis with the experimental data--Volumetric strains for the mix of f_{cy}= 33MPa--

Figs 7 to **10** show calculated results together with experimental results for the purpose of comparison. An initial set of values for calculation was:

$\sigma'_1=0.9f_{cy}$, $\sigma'_2=0.0$, $\varepsilon'_1=0.003$, $\varepsilon'_2=0.0$

where σ'_1 and ε'_1 are axial stress and strain respectively, σ'_2 and ε'_2 are hoop stress and strain respectively.

The incremental step of axial strain was set to $d\varepsilon'_1=10.0\times10^{-6}$, which is small enough to confirm the accuracy of the calculation. The calculation was terminated when the stress state of concrete reached the ultimate strength envelope. In the experiments[2)], the stress path moves towards the inside of the ultimate strength envelope after it reaches the strength envelope. This means that the strength envelopes shrink with the increase of plastic deformation. This process cannot be pre-

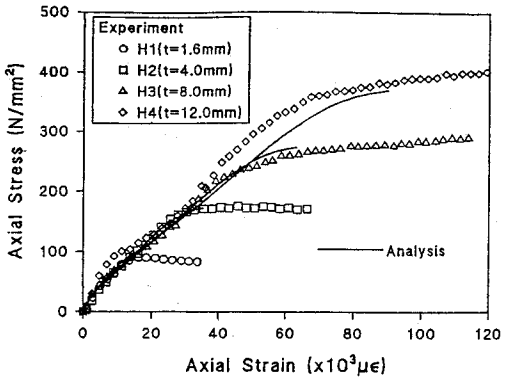

Fig.9 Comparison of analysis with the experimental data--Stress-strain curves for the mix of f_{cy} =45MPa--

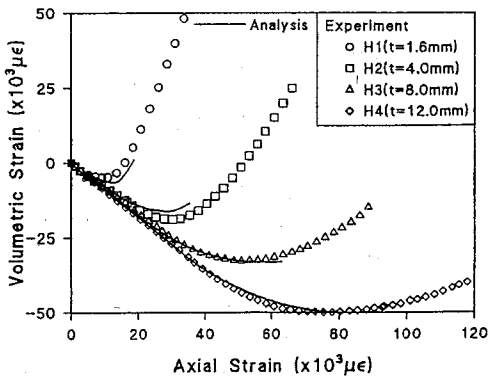

Fig.10 Comparison of analysis with the experimental data--Volumetric strains for the mix of f_{cy}= 45MPa--

dicted by the proposed constitutive model, as it is no longer a work-hardening process from the viewpoint of the classical plasticity theory even if the axial stress increases.

The overall behaviours predicted by the proposed model reproduce the experimental results very well. Consequently, the proposed model established in the present paper by using the work-hardening plasticity theory has proved to yield a good approximation to the test results.

4. FE analysis code for confined concrete

In order to analyse general forms of confined concrete structures, the proposed model for post-OUFP concrete is incorporated into the FE analysis program previously developed at Imperial College by Gonzalez-Vidosa, Kotsovos and Pavlović[4),5)]. This uses Kotsovos's constitutive model, and may be employed to analyse ordinary RC or PC structures made of either normal- or high-strength mixes.

Because the Kotsovos model is not capable of representing the dilational behaviour of concrete beyond the OUFP level, the existing FE analysis mentioned in the preceding paragraph cannot predict the ductile behaviour of confined concrete in which significant confining pressure is developed due to the dilational behaviour of concrete. For the purpose of analysing such confined concrete structures (in particular composite structures with concrete being encased in a steel shell), the appropriate FE analysis code is now developed by using the proposed model for the post-OUFP behaviour, thus expanding the range of problems which the existing FE analysis covers to encompass such composite construction.

As the available experimental information obtained from the tests is very limited, the resulting model is as yet incomplete. Therefore, a number of assumptions are required for incorporation into the proposed model with the FE analysis code at this stage.

The constitutive relations for the post-OUFP behaviour have been investigated only for such axisymmetric stress states for which the Lode angle (θ) equals 60°, (i. e., $\sigma'_1>\sigma'_2=\sigma'_3$). The effect of varying the Lode angle is as yet unknown and the proposed model is assumed to be independent of θ. In order that the proposed model may be incorporated within the existing model without any contradiction, the stress-strain relationship and ultimate strength envelope of the existing model should also be assumed to be independent of the Lode angle. However, while the Kotsovos model describing the deformational response of concrete is independent of the Lode angle , the ultimate strength (US) envelope of the existing model is dependent on the Lode angle. The effect of varying the Lode angle is assumed to be interpolated by using the values at $\theta=60°$ and $\theta=0°$. In order to make the existing US envelope reasonably compatible with the proposed post-OUFP model, the following expression for the US envelope is adopted;

$$\tau'_0/f_{cy}=0.944\ (\sigma'_0/f_{cy}+0.05)^{0.724} \quad \cdots\cdots\cdots\cdots\cdots\cdots (32)$$

which means that the value at $\theta=60°$ of the US envelope is assumed to be valid independently of the Lode angle. The ultimate strength of concrete at $\theta=60°$ is larger in the octahedral stress space than that at $\theta=0°$. Therefore, it should be noted that the above assumption may lead to the overestimation of load-carrying capacity or the delay of crack formation when the stress state of a concrete element is actually around $\theta=0°$. On the other hand, for most of the usual confined con-

crete structures, such as concrete-filled steel tubes, the maximum compressive principal stress is much larger than the other two principal stresses in the critical regions of these structures (for example, the compressive region of columns and beam). Therefore, the Lode angles of the stress states in such regions are expected to be around $60°$. Consequently it is expected that the above simplified assumption will affect the overall behaviour very little in most of the usual confined concrete structures.

In a tension region, i.e., where at least one principal stress is tensile, the Kotsovos model is used to describe the stress-strain relationships. When the ultimate strength envelope expressed as equation (32) is exceeded in tension, a cracked plane is assumed to form. The treatment of the crack is the same as the procedure mentioned elsewhere[4),5)].

In a compression region, i.e., where all three principal stresses are compressive, the Kotsovos model is used before the OUFP level. After the stress state at a Gauss point exceeds the OUFP level in compression, the proposed model for the post-OUFP behaviour of concrete is used to depict the concrete behaviour at the Gauss point. The OUFP envelope is assumed to be adequately defined by the following expression:

$$\tau_0'/f_{cy}=0.961\ \{0.944\ (\sigma_0'/f_{cy}+0.05)^{0.724}\} \quad \cdots\cdots(33)$$

which under uniaxial compression has a value equal to 90% of the cylinder strength. Once the concrete element exceeds the OUFP level, the proposed model is used for the rest of the analysis, which implies that concrete has been irreversibly changed to the different material with the properties of the proposed model (which may be called"the post-OUFP concrete").

After the concrete element is transformed to the post-OUFP behaviour, the stress state is calculated from given strains by using the plasticity-based constitutive model proposed in equation (31) in the previous section. In addition, it is assumed that no tensile stress is developed in the concrete element once the latter is transformed into the post-OUFP concrete model; i.e., any tensile stress is ignored while its effect is redistributed. This assumption is supported by the experimental evidence obtained by Ďelibes-Liniers[6)], who suggested that the tensile strength of concrete was significantly reduced after concrete was compressed beyond 90% of its uniaxial strength.

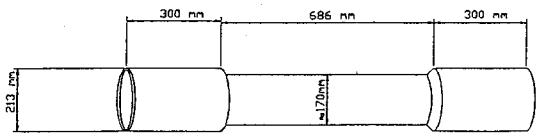

Fig.11 Test specimens of circular section prior to their being filled with concrete[7)]

5. FINITE-ELEMENT ANALYSIS OF CONCRETE-FILLED STEEL TUBES SUBJECTED TO ECCENTRIC LOADING

Concrete-filled steel tubes are analysed in order to verify the validity of the developed FE analysis code by comparing the analysed results with existing experimental data. Concrete-filled composite columns are chosen as examples for this purpose, because a relatively large confining pressure is considered to develop in regions within such structures, and because reliable experimental data on these structure types have been published. Most of the published works available on concrete-filled composite columns are empirical and/or semi-empirical studies. As far as the authors are aware, few FE analyses on such structures have been published. Therefore, it is both interesting and challenging to analyse such structures by the present FE model.

(1) Description of the testing

Sen[7)] carried out a series of experiments to investigate the moment-curvature relationships of short columns of circular section (subsequently filled with concrete) when subjected to axial loading and end moments. The testing described in Sen's work may be summarized as follows:

a) Specimen

The specimen used is illustrated in **Fig.11**. It was 686mm long and 170mm in diameter. A 300mm long, 213mm diameter, 32mm thick tube was welded on to each end of the test specimen for clamping purposes. The total length of 1235mm was then filled with concrete.

b) Experimental procedure

The axial load was increased until a pre-assigned value, at which it was kept constant for the rest of the test. After this constant axial load was reached, a continuously increasing moment was applied to the ends of the specimen.

(2) Finite-element analysis

Nine (9) cases were analysed for the comparison with the reported experimental results obtained in Sen's work. Two thicknesses of steel

Table 3 Dimension and material properties of test specimens

<Group A>

Case	Axial Load N (kN)	Outside Diameter D (mm)	Thickness of tube t (mm)	Yield stress f_y (N/mm^2)	Young's modulus E_s (N/mm^2)	Cube strength f_{cu} (N/mm^2)
A-1	118	169.469	10.058			57.78
A-2	588	169.469	10.084			54.88
A-3	980	169.291	10.135	318.991	206,736	61.16
A-4	1470	169.266	10.109			54.88
A-5	1960	169.433	10.135			57.50
Average		169.388	10.104	318.991	206,736	57.24

<Group B>

Case	Axial Load N (kN)	Outside Diameter D (mm)	Thickness of tube t (mm)	Yield stress f_y (N/mm^2)	Young's modulus E_s (N/mm^2)	Cube strength f_{cu} (N/mm^2)
B-1	60	168.021	5.232			54.47
B-2	490	168.046	5.369	350.890	198,534	52.33
B-3	980	167.970	5.283			50.60
B-4	1470	167.996	5.283			54.06
Average		168.036	10.104	318.991	206,736	52.87

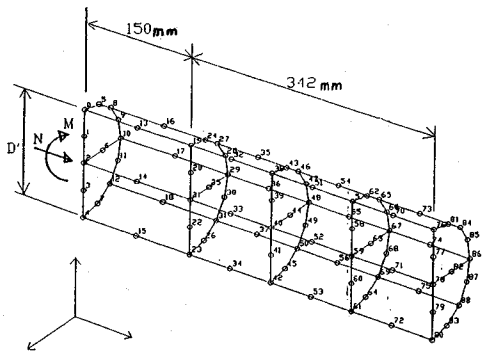

Fig.12 Finite-element mesh for concrete-filled circular section

tube were chosen for such a comparison. Dimensions and material properties of the experimental cases of interest are tabulated in **Table 3.**

In the present analyses, steel shells are modelled as membrane elements. Geometrical non-linearity is considered by using the Total-Lagrangian technique. The finite-element mesh for the analysis is shown in **Fig.12.** Only one fourth of the specimen was modelled on account of symmetry. It was assumed that external forces such as axial load and moment were applied at the centre of the clamped portion of the specimen. Therefore, only one half of the clamped portion was modelled in the analysis (see **Fig.12**). The "clamped" portion of the FE model (i. e., the portion prevented from translating, but still allowing freedom of rotation) was reinforced by steel stiffeners with larger

Table 4 Dimensions and material properties used for the FE analysis

Case	Axial Load N (kN)	Concrete Diameter D' (mm)	Thickness of tube t' (mm)	Yield stress f_y (N/mm^2)	Young's modulus E_s (N/mm^2)	Cylinder strength f_{cy} (N/mm^2)
A-1	118					
A-2	588					
A-3	980	149.2	10.78	319.0	206,736	48.7
A-4	1470					
A-5	1960					
B-1	60					
B-2	490	157.4	5.52	350.9	198,534	45.0
B-3	980					
B-4	1470					

Young's modulus to make sure that the specimen would not fail at the clamped portion (this simulated the effect of the thicker and larger diameter tube which was welded for clamping purposes in the experiment). Dimensions and material properties adopted for the analysis are tabulated in **Table 4.** The average values of each group in **Table 3** were used in the analysis. The diameter of the meshed model was set equal to the inside diameter of the steel tube, because the behaviour of concrete was of particular interest and was considered to dominate the overall behaviour of the structure after the yielding of the steel. The thickness of the membrane element for the steel tubes was adjusted so that the section area became equal to that of the tested steel tube. The cylinder strength of the concrete (f_{cy}), which was used in the analysis, was calculated from the cube tested strength (f_{cu}) as $f_{cy}=0.85f_{cu}$. Because the cylinder strength of the concrete was around 45N/mm^2 (i. e., 48.7N/mm^2 for group A and 45.0N/mm^2 for group B), the proposed model with material constants established in the previous section for the mix of f_{cy}=45N/mm^2 was used for the analysis. The stress-strain relation of steel was assumed to be adequately modelled by the elastic-perfectly plastic model which was subject to the Von-Mises yield criteria.

(3) Comparison between experimental and analytical results

Moment-curvature curves obtained from both the experiments and the analyses are shown on **Figs.13** and **14**, where the numbers in the boxes represent the axial load (in kN) applied prior to the moment. **Fig.13** is for group A (i.e., steel thickness t=10.0mm) and **Fig.14** for group B (i.e., t=5.0mm).

The experimental curves exhibit a fairly linear moment-curvature relation in the earlier part, before the yielding of the steel, and then this is

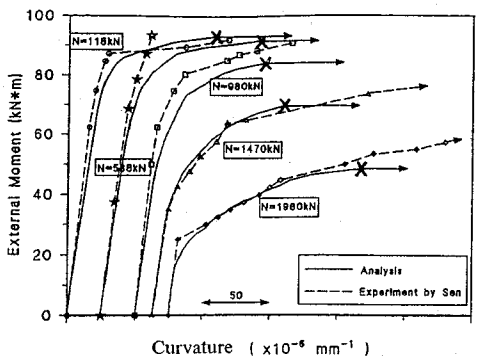

Fig.13 Comparison of experimental and analytical moment–curvature relationships (Group A)

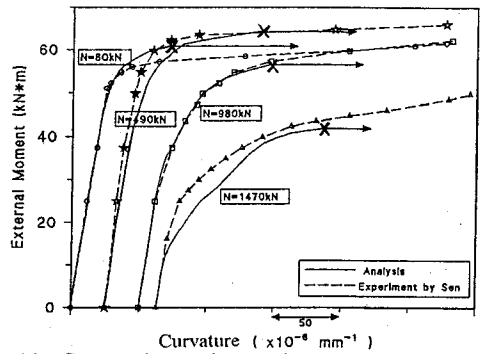

Fig.14 Comparison of experimental and analytical moment–curvature relationships (Group B)

followed by a pronounced deviation from linearity. The curves, particularly those with high axial load, do not show a flat plateau. There follows a further ascending branch, whose gradient is fairly linear or even shows a slight increase in the stiffness. **Fig.15** shows typical load–strain curves for concrete–filled columns, which are extracted from Ref 8). The present moment–curvature relation corresponds to the type of curve depicted in **Fig. 15 (b)** . Such a characteristic feature of load–strain or load–displacement curves is sometimes observed in short composite structures, in particular those with concrete being encased in relatively thick steel tubes. Some researchers[8),9)] take a view that the load at the point of inflection, where $\partial^2 N/\partial \varepsilon^2 = 0$ as in **Fig.15 (b)**, is to be regarded as the ultimate load, because there is no other characteristic feature beyond this point, and because the deformation of the member beyond this point may be too large to suit the normal use of structures. A similar phenomenon was observed in the experiment reported in Ref 2). According to the analysis of this experimental data as discussed there, the last ascending branch may be attributed to the post–ultimate strength behaviour of concrete and/or the strain–hardening of the steel tube. Therefore, the inflection point in the moment–curvature curve is considered to be the point where concrete reaches the ultimate strength envelope.

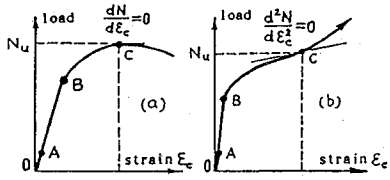

Fig.15 Typical load–strain curves of short concrete–filled composite columns[8)]

Figs.13 and **14** indicate that the curves obtained from the FE analysis mimic the experimental curves very well up to the ultimate load in accordance with the above definition. The last converged load step, which is represented by a crossed point in the plots, is considered to be very close to the ultimate load of the above definition (i. e., the inflection point). The ascending branches beyond such ultimate loads cannot be predicted by the analysis, where the solution does not converge, because neither the post–ultimate strength behaviours of concrete nor the strain–hardening of the steel tube are considered in the present analyses. In view of this, the proposed FE analysis predicts the deformational response of the present structures very accurately, which proves that the proposed constitutive model is very accurate, for practical purposes, in analysing confined concrete structures. In addition, according to the above discussion on the definition of the ultimate load, it is reasonable to consider the ultimate load obtained from the present FE analysis as the practical ultimate load of the structures.

Consequently, the present FE analysis could provide a reliable tool for the accurate prediction of the ultimate load and deformational response of structural members such as those presently considered.

6. CONCLUSION

The post–OUFP behaviour of concrete was successfully modelled by using the classic work–hardening plasticity theory. The characteristic features of the proposed plasticity model may be described as follows:

(1) In order to express the sensitivity of the ductility to hydrostatic pressure, the idea of the Cap–models, where the loading function consists of the ultimate strength envelope and the cap function, are used.

(2) In order to express the volume change of

the post-OUFP behaviour of concrete accurately, the non-associated flow rule is used, in which the plastic potential function is defined independently of the loading function.

However, it should be noted that, due to the limitation of the plasticity theory, the behaviour was modelled only up to the ultimate states, i. e., until the stress state intersects the ultimate strength envelope. In order to model the post-ultimate-state behaviour, other theoretical bases such as, for example, the strain-space plasticity theory are needed.

A finite-element program was developed in order to analyse general forms of confined concrete structures and, in particular, composite structures with concrete being encased in a steel shell. The ensuing FE program successfully predicted the load-carrying capacity and deformational response of eccentrically loaded concrete-filled steel tubes. As far as the authors know, the deformational behaviour of such eccentrically loaded composite columns, where significant development of confining pressure is observed, had never been successfully predicted until the present work by 3 D-FE analysis, in which confinement effects are directly assessed by using general constitutive relations of concrete.

In the present work, constitutive relations for only two mixes were investigated. A wide variety of mixes (in particular, with respect to the cylinder strength) should be investigated in future. In addition, the proposed model still has many material parameters to be determined for each mix of concrete. Therefore, the effect on the material parameters of the proposed model which the cylinder strength or other factors of mixes have should be clarified and empirically expressed as mathematical equations in future work.

Although the application of the proposed model to FE analysis is still very limited due to both theoretical limitations and limited experimental information available, the successful predictions of the behaviour of the confined concrete structures outlined in the present paper implies that the authors' approach was appropriate in that the dilational and ductile behaviour of concrete should be accurately modelled exclusively on experimental information obtained from tests in which concrete has been subjected to passive confinement, with the information describing concrete behaviour beyond OUFP being of particular interest.

Notations

(1) Expression of tensor

The summation convention is adopted for expressing tensor equations in the present paper. δ_{ij}; Kronecker's delta (i.e., $\delta_{ij}=1$ *if* $i=j$, $\delta_{ij}=0$ *if* $i\neq j$)

(2) Stress and strain

Note that compressive stresses and strains in concrete are usually defined to be positive for convenience; such stresses and strains in the system where compression is defined to be positive are represented by the dashed notations.

σ (σ_i, σ_{ij}); Stress (conponent of stress vector and tensor)

ε (ε_i, ε_{ij}); Strain (conponent of strain vector and tensor)

σ_0; Octahedral normal stress which is defined as $\sigma_0=(\sigma_{11}+\sigma_{22}+\sigma_{33})/3$

s_{ij}; Deviatoric stress tensor which is defined as $s_{ij}=\sigma_{ij}-\sigma_0\delta_{ij}$

τ_0; Octahedral shear stress which is defined as $\tau_0=(s_{ij}s_{ij}/3)^{1/2}$

ε_0; Octahedral normal strain which is defined as $\varepsilon_0=(\varepsilon_{11}+\varepsilon_{22}+\varepsilon_{33})/3$

e_{ij}; *Deviatoric strain tensor which is defined as* $e_{ij}=\varepsilon_{ij}-\varepsilon_0\delta_{ij}$

γ_0; Octahedral shear strain which is defined as $\gamma_0=(e_{ij}e_{ij}/3)^{1/2}$

θ; Lode angle or angle of similarity which is defined as $\cos 3\theta=\sqrt{2}s_{ij}s_{jk}s_{ki}/3\tau_0^3$

σ^e, ε^e; Elastic portion of stress and strain respectively

σ^P, ε^P; Plastic portion of stress and strain respectively

(3) Material constants and parameters

E; Young's modulus

ν; Poisson's ratio

f_{cy}; Cylinder strength of concrete

f_{cu}; Cube strength of concrete

f_y; Yield stress of steel

K_e; Elastic bulk modulus

G_e; Elastic shear modulus

(4) Plasticity theory

f ( ); Loading function

g ( ); Plastic potential function

P; Hardening parameter

W^P; Plastic work which is defined as $dW^P=\sigma_{ij}d\varepsilon_{ij}^P$

REFERENCES

1) Kotsovos, M. D. and Perry, S. H.: Behaviour of concrete subjected to passive confinement, Materials and Structures, RILEM, Vol. 19, pp. 259-264, 1986.
2) Kinoshita, M., Kotsovos, M. D. and Pavlović, M. N.: Behaviour of concrete under passive confinement, Proc. of JSCE, No. 502/V-25, 1994.
3) Chen, W. F.: Plasticity in Reinforced Concrete, McGraw-Hill, New York, 1982.
4) Gonzalez-Vidosa, F., Kotsovos, M. D. and Pavlović, M. N.: A three-dimensional nonlinear finite-ele-

ment model for structural concrete– (part1) main features and objectivity study, Proc. Instn Civ Engrs (Part2), Vol. 91, pp. 517–544, 1991.
5) Gonzalez–Vidosa, F., Kotsovos, M. D. and Pavlović, M. N.: A three–dimensional nonlinear finite–element model for structural concrete– (part2) generality study, Proc. Instn Civ Engrs (Part2), Vol. 91, pp. 545–560, 1991.
6) Delibes–Liniers, A.: Microcracking of concrete under compression and its influence on tensile strength, Materials and Structures, RILEM, Vol. 20, pp. 111–116, 1987.
7) Sen, H. K.: Triaxial effects in concrete–filled tubular steel columns, PhD thesis, University of London, 1969.
8) Cai, S. H.: Ultimate strength of concrete–filled tube columns, Composite Construction in Steel and Concrete, ASCE, pp. 702–727, 1988.
9) Shang–Tong, Z and Ruo–Yu, M.: Stress–strain relationship and strength of concrete–filled tubes, Composite Construction in Steel and Concrete, ASCE, pp. 773–785, 1988.

(Received January 10, 1994)

受働的拘束を受けるコンクリートの構成モデルとその構造解析における適用

木下雅敬・ミリヤ パブロビッチ・マイケル コツボス

コンクリート充填鋼管等では，コンクリートが鋼材により拘束されることにより，その強度及びダクティリティーが大きく改善される．本文では，このような受働的な拘束を受けるコンクリートの構成モデルを提案している．また，提案された構成モデルを組み込んだFEM解析コードを開発し，偏心圧縮を受けるコンクリート充填鋼管の挙動を解析した結果，解析結果は実験結果をうまく再現している．